Temporal Postural Synergies of the Hand in Rapid Grasping Tasks

Ramana Vinjamuri, *Member, IEEE*, Mingui Sun, *Senior Member, IEEE*, Cheng-Chun Chang, *Member, IEEE*, Heung-No Lee, *Member, IEEE*, Robert J. Sclabassi, *Senior Member, IEEE*, and Zhi-Hong Mao, *Senior Member, IEEE*

***Abstract*—Postural synergies of the hand have been widely proposed in the literature, but only a few attempts were made to visualize temporal postural synergies, i.e., profiles of postural synergies varying over time. This paper aims to derive temporal postural synergies from kinematic synergies extracted from joint angular velocity profiles of rapid grasping movements. The rapid movements constrain the kinematic synergies to combine instantaneously, and thus, the movements can be approximated by a weighted summation of synchronous synergies. After being extracted by using singular value decomposition, the synchronous kinematic synergies were translated into temporal postural synergies, which revealed strategies of enslaving, metacarpal flexion for larger movements, and hierarchical recruitment of joints, adapted by subjects while grasping.**

***Index Terms*—Brain–computer interface (BCI), grasping, kinematic synergies, postural synergies, rehabilitation, virtual reality.**

I. Introduction

THE CONCEPT of synergies (in Greek *synergos* means working together) received the first numerical representation as a possible solution to the DOF problem by Bernstein [1]. Although synergies were originally defined by Bernstein as high-level control of kinematic parameters, different definitions of synergies exist and the term has been generalized to indicate the common patterns observed in the behaviors of muscles, joints, forces, actions, etc. Synergies in hand movements especially present a complex optimization problem as to how the central nervous system (CNS) controls the hand with over 25 DOF [2]. However, the CNS handles all the movements effortlessly, and at the same time, dexterously. Endeavoring to solve the DOF problem, many researchers have proposed numerous concepts of synergies, which are as follows.

1) *Postural synergies:* Researchers found that the entire act of grasp can be described by a small number of dominant postures, which were defined as postural synergies [3]–[8].
2) *Kinematic synergies:* Studies in [9] and [10] expressed the angular velocities of finger joints as linear combinations of a small number of kinematic synergies, which were also angular velocities of finger joints, but were extracted from a large set of natural movements. Kinematic synergies are not limited to hand movements. d'Avella *et al.* [11] reported that kinematic synergies were found in tracking 7-DOF arm movements.
3) *Dynamic synergies:* Dynamic synergies were defined as stable correlations between joint torques that were found during precision grip movements in [9]. In addition to synergies proposed in postures, kinematics, and dynamics, which are of relevance to the current study, synergies were also proposed in muscle activities [11].

In this paper, we consider both kinematic synergies (which are shared spatiotemporal patterns in the joint angular velocity profiles of hand movements [10]) and temporal postural synergies (which present shared patterns of postural variations over time). This paper undertakes two tasks. The first task is to investigate rapid hand movements to extract kinematic synergies. Based on a convolutive-mixture model for generation of hand movements (see Section II-A), we propose that a kinematic synergy is the production of impulse responses of a set of filters that characterize the related neural–biomechanical structures responsible for the movement of finger joints in response to a command impulse (see Section II-A). Based on this model, synchronous synergies can be computed from rapid grasping tasks using singular value decomposition (SVD). This is different from the method used in our previous study [10], which iteratively searched for both the shaping and timing of kinematic synergies simultaneously. In this paper, we concentrate on determining the morphology of kinematic synergies. In the future, the obtained synergies will be used as templates to decompose the hand movements, to show how the kinematic synergies are recruited in movement generation.

The second task of this paper is to translate the obtained kinematic synergies into temporal postural synergies. This method for computing temporal postural synergies can be applied to brain–computer interface (BCI) and rehabilitation. Eigenpostures or postural synergies were reported to have physiological and anatomical significances [4], [8]. In [12] and [13], it was proposed that motor disabilities in individuals with stroke might

Manuscript received December 29, 2008; revised August 30, 2009; accepted December 6, 2009. Date of publication January 12, 2010; date of current version July 9, 2010. This work was supported by the National Science Foundation under Grant CMMI-0727256.

R. Vinjamuri is with the Department of Physical Medicine and Rehabilitation, University of Pittsburgh, Pittsburgh, PA 15213 USA (e-mail: rkv3@pitt.edu).

M. Sun is with the Department of Neurological Surgery, the Department of Electrical and Computer Engineering, and the Department of Bioengineering, University of Pittsburgh, Pittsburgh, PA 15213 USA (e-mail: mrsun@neuronet.pitt.edu).

C.-C. Chang is with the Department of Electrical Engineering, National Taipei University of Technology, Taipei 106, Taiwan (e-mail: ccchang@ntut.edu.tw).

H.-N. Lee is with the Department of Information and Communications, Gwangju Institute of Science and Technology, Gwangju 500-712, Korea (e-mail: heungno@gist.ac.kr).

R. J. Sclabassi is with the Computational Diagnostics Incorporated, Pittsburgh, PA 15213 USA (e-mail: bobs@cdi.com).

Z.-H. Mao is with the Department of Electrical and Computer Engineering, and the Department of Bioengineering, University of Pittsburgh, Pittsburgh, PA 15261 USA (e-mail: maozh@engr.pitt.edu).

Color versions of one or more of the figures in this paper are available online at http://ieeexplore.ieee.org.

Digital Object Identifier 10.1109/TITB.2009.2038907

be due to missing synergies found in unimpaired individuals. Study of the synergies in normal subjects and comparing them with synergies in individuals with movement disorders will have significant contribution to rehabilitation. By training in virtual environments and by graphical visualization of temporal postural synergies, if lacking synergies are learnt by individuals with motor disabilities, it might be possible to bring them back to normal motor behaviors. Virtual reality environments are already under use for rehabilitation of individuals with motor disabilities due to stroke [13]. Such virtual platforms for rehabilitation can be greatly enhanced with the addition of graphical visualization of temporal postural synergies.

With the advent of virtual reality in recent years, postural synergies have been extensively explored, but only a few attempts were made to visualize postural synergies across time [3], [5], [8]. Many matrix factorization methods such as principal component analysis (PCA), SVD, and linear discriminant analysis (LDA) have been used to obtain a few dominant postures over a wide range of postures collected during reach-and-grasp experiments. But, these were all static postures. The earlier attempts [4], [5], [8] were limited to estimation by extrapolation of eigenpostures or PC postures. In [8], postural variation across time was obtained, but was estimated by adding a weighted component of variation to a mean posture. In [4] and [5], similar computations were carried out. In contrast, temporal postural synergies presented in this paper are not static postures, but are postural variation patterns observed across time.

The rest of this paper is organized as follows. Section II presents a summary of methods, which include descriptions for 1) a convolutive-mixture model of movement generation, and how this model is used to interpret rapid hand movements as superpositions of synchronous kinematic synergies; 2) the materials used in the human experiment; 3) the procedure of the experiment; and 4) our proposed algorithm for extraction of kinematic synergy and calculation of temporal postural synergies. Section III shows the results of the human experiment and data analysis. Section IV presents a discussion on the results and significance of our study. The last section is the conclusion.

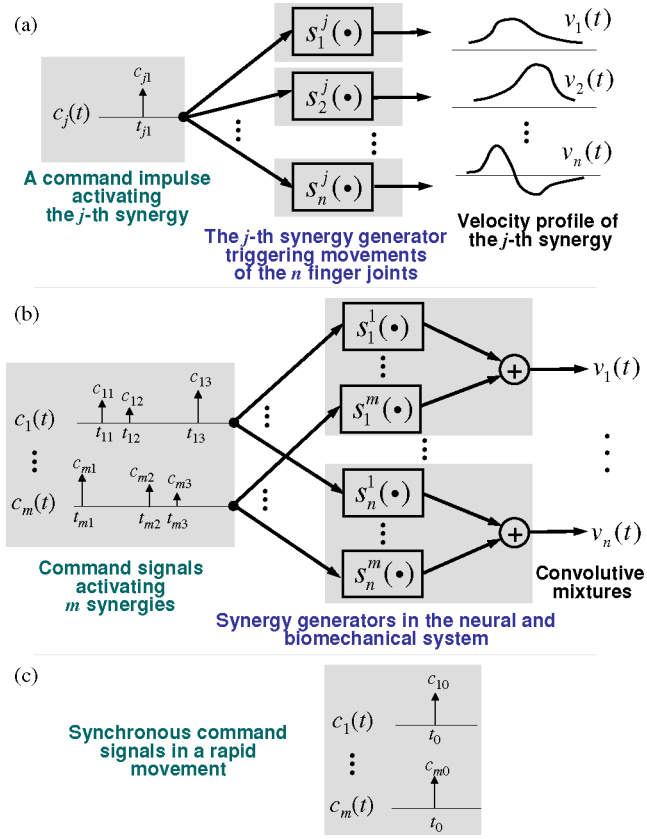

Fig. 1. Convolutive-mixture model for hand movement generation. (a) A kinematic synergy can be viewed as impulse responses of a set of filters that summarize the related neural–biomechanical structures triggering finger joint movements in response to an impulse in the higher level neural system. (b) A movement profile of the hand can be modeled as convolutive mixtures of command impulses passing through the corresponding filters or synergy generators [14]. (c) A rapid movement is achieved as a weighted sum of synchronous synergies.

II. Methods

A. Model

Following [14], we model the angular velocities of finger joints as convolutive mixtures of some command signals represented by impulse trains (see Fig. 1). Let us start with the simplest case where a command signal contains only a single impulse. Such an impulse originates in the higher level neural system, then activates some circuits in the lower level neural system, and finally, stimulates certain biomechanical structures. This process creates a stereotyped angular change at the finger joints of the hand. We can view this process as the activation of a *kinematic synergy* in hand movements [see Fig. 1(a)], which is similar to the production of impulse responses of a set of filters (or synergy generators). The output of each filter corresponds to the movement of a specific finger joint. We assume that all the filters are linear finite-impulse response (FIR) filters. Under such an assumption, when the command signal is a train of impulses, a movement profile of the hand can be expressed as the superposition of the impulse responses of the command impulses passing through the corresponding filters residing in the neural system and connected biomechanical system [see Fig. 1(b)]. Although the neuromuscular system is nonlinear, considering a linear approximation might give useful insight of the system. Moreover, it has been suggested that motor behavior of vertebrates can be well approximated by linear combination of tiny modules of movement called movement primitives [15], [16].

Based on the aforementioned model, a kinematic synergy can be depicted as impulse responses of a set of filters, denoted by $\mathbf{s}^j(t) \equiv [s_1^j(t), \ldots, s_n^j(t)]'$ for the jth synergy, where $'$ represents transpose and n is the total number of the considered joints of the hand. When the jth synergy is activated at time t_{j1} with amplitude c_{j1} (in other words, the jth synergy generator is activated by an impulse with amplitude c_{j1} at time t_{j1}) [see Fig. 1(a)], a hand movement is generated with the following angular velocity profile:

$$\mathbf{v}(t) = c_{j1}\mathbf{s}^j(t - t_{j1})$$

where $\mathbf{v}(t)$ denotes $[v_1(t), \ldots, v_n(t)]'$ and $v_i(t)$ $(i = 1, \ldots, n)$ represents the angular velocity of the ith joint of the hand at time

t. When the jth synergy generator is activated by a command signal $c_j(t)$ containing a train of impulses, with amplitudes c_{jk} at times t_{jk} [$k = 1, \ldots, K_j$; K_j is the total number of impulses in $c_j(t)$], the angular velocity profile of the finger joints becomes

$$\mathbf{v}(t) = (c_j * \mathbf{s}^j)(t) = \sum_{k=1}^{K_j} c_{jk}\mathbf{s}^j(t - t_{jk})$$

where $*$ represents convolution. The aforementioned equation can also be written as follows:

$$v_i(t) = \sum_{k=1}^{K_j} c_{jk} s_i^j(t - t_{jk}), \qquad i = 1, \ldots, n.$$

When more than one synergies are considered [see Fig. 1(b)], our model can be expressed by the following equation:

$$\begin{aligned}\mathbf{v}(t) &= \sum_{j=1}^{m}(c_j * \mathbf{s}^j)(t) \\ &= \sum_{j=1}^{m}\sum_{k=1}^{K_j} c_{jk}\mathbf{s}^j(t - t_{jk}) \end{aligned} \tag{1}$$

or

$$v_i(t) = \sum_{j=1}^{m}\sum_{k=1}^{K_j} c_{jk} s_i^j(t - t_{jk}), \qquad i = 1, \ldots, n$$

where m is the total number of synergies under consideration. A similar model was successfully used in the extraction of sources of tremor from hand joint movements of patients with movement disorders [14].

Compared with the time-varying synergy model proposed in our previous work [10], the current model (1) allows repetitive uses of synergies in a single movement. Although this is physiologically more plausible, the decomposition of synergies becomes more difficult from computational point of view. We need to determine not only the shapes of the synergies, but also their onset times, amplitudes, and number of recruitments in the movement. Instead of iteratively adjusting both the shaping and timing of the synergies simultaneously, we propose to take two steps. The first step is to determine the morphology of synergies, and the second step is to use the obtained synergies as templates or basis functions to decompose the hand movements. In this paper, we concentrate on the first step by investigating rapid movements, and in another manuscript, we study the second step based on l_1 minimization [17].

In this paper, we only consider rapid grasps. We asked the human subjects to perform the rapid grasps imitating as though reacting to instantaneous impulses descending from the CNS (see Section II-C). We assume that these rapid movements minimize the reaction times and constrain the synergies to combine almost instantaneously, i.e., all impulses from the CNS arrive at the filters or synergy generators at approximately the same time [see Fig. 1(c)]. Thus, a rapid movement can be achieved as a weighted summation of *synchronous* synergies, as expressed in the following equation:

$$\mathbf{v}(t) = \sum_{j=1}^{m} c_{j0}\mathbf{s}^j(t - t_0) \tag{2}$$

where the impulses of $c_j(t)$, $j = 1, \ldots, m$, occur at the same time t_0, but may have different amplitude c_{j0}.

We use superscript g ($g = 1, 2, \ldots$) in $\mathbf{v}^g(t)$ to distinguish angular velocity profiles of different grasping tasks. If we shift all $\mathbf{v}^g(t)$ in time such that the movement onset times coincide with $t = 0$, then the time of impulses t_0 in $\mathbf{v}^g(t)$ should be the same for all g, but the amplitudes of impulses, denoted as c_{j0}^g, may be different for different g. Therefore, for grasping task g, (3) can be rewritten as follows:

$$\mathbf{v}^g(t) = \sum_{j=1}^{m} c_{j0}^g\mathbf{s}^j(t - t_0) \tag{3}$$

or

$$v_i^g(t) = \sum_{j=1}^{m} c_{j0}^g s_i^j(t - t_0), \qquad i = 1, \ldots, n. \tag{4}$$

Section II-D will show how to use SVD to extract the synchronous kinematic synergies, precisely, $\mathbf{s}^j(t - t_0)$, a shifted version of $\mathbf{s}^j(t)$.

B. Materials

In the experiment, we used a CyberGlove [18] equipped with 22 sensors that captured hand movements at a maximum frequency of 86 Hz. For the purpose of reducing computational burden, we only considered 15 of the sensors, which measure the angles of the carpometacarpal (CMC), metacarpophalangeal (MCP), and interphalangeal (IP) joints of the thumb and the MCP, proximal interphalangeal (PIP), and distal interphalangeal (DIP) joints of the other four fingers. These 15 joints can capture most characteristics of the hand in grasping tasks. We used several objects of different shapes (spheres, circular discs, rectangles, pentagons, nuts, and bolts) and different dimensions (spheres: 1–5 cm in radius, discs: 2–10 cm in radius, rectangles and pentagons: 1–3 cm each side, nuts and bolts: 2–5 cm in length) in the grasping tasks. We selected these objects based on two strategies: one was using different shapes, and the other was gradually increasing sizes of similar shaped objects. Some similar-shaped objects were intentionally used to observe trends in grasping movements.

C. Experiment

An experiment consisted of tasks of grasping the objects of various shapes and sizes. During the experiment, the subject was in a seated position, resting his/her right hand at a corner of a table before the start of a grasping task. We used computer-generated beeps to signal start and stop times of a task. In each task, the subject grasped the object placed on the table upon hearing the start beep and held it until the stop beep. We asked the subject to perform the grasp rapidly (as though reacting to instantaneous impulses descending from the CNS). Each task lasted for 1.6 s, although the actual movement lasted for less

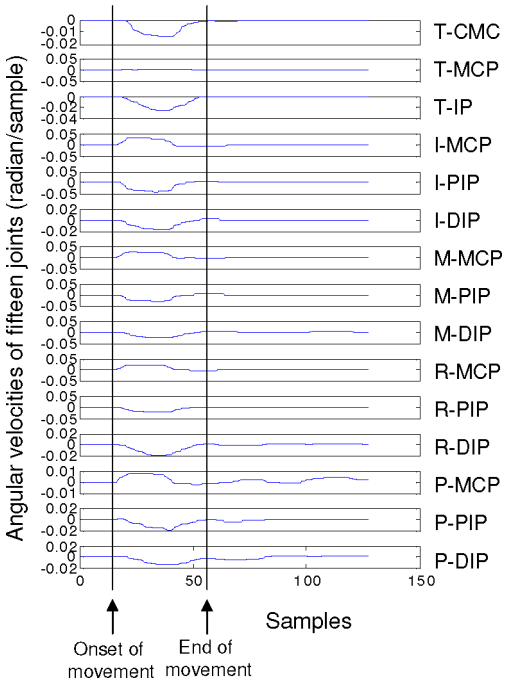

Fig. 2. Sample of movement profile (finger-joint angular velocity profile). Onset and end of movements are marked in the figure. T, thumb; I, index finger; M, middle finger; R, ring finger; and P, pinky finger; CMC, carpometacarpal joint; MCP, metacarpophalangeal joint; IP, interphalangeal joint; PIP, proximal interphalangeal joint; DIP, distal interphalangeal joint.

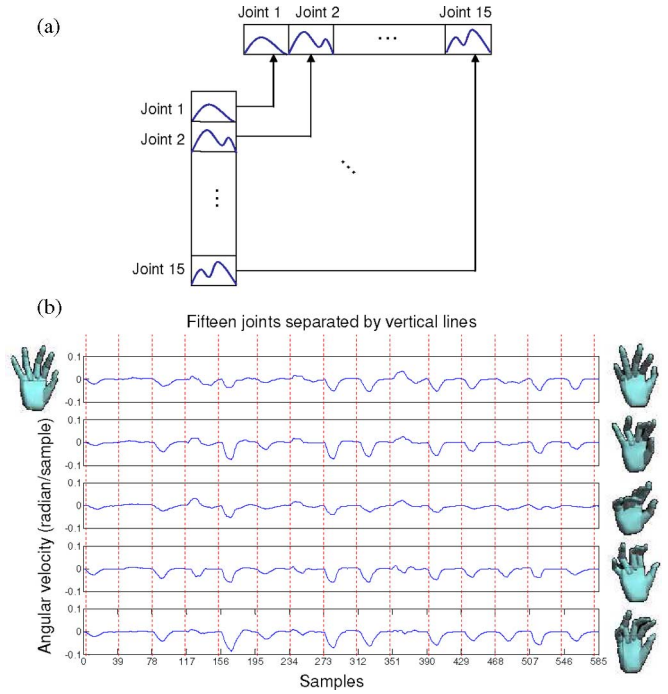

Fig. 3. Angular velocity matrix. (a) Cascading angular velocity profiles of 15 joints to form a row of the anuglar velocity matrix. (b) Each row of the angular velocity matrix represents a grasping task. This is a transformation of the (left) initial posture (left) to (right) final posture). In each row, the angular velocity profiles of 15 joints are separated by dotted red lines. Five such tasks are depicted here.

than half a second. Duration of 1.6 s was used in order to make sure that all subjects complete the movement successfully. It also helped the subjects, who had delayed responses after the beep. Throughout the experiment, we used the CyberGlove to record joint angles. We first asked each subject to perform 40 rapid grasping tasks, which formed the training data used to obtain synergies. After a short recess of about 3–4 min, we collected 20 more tasks by picking 20 objects in a random order, irrespective of their shapes and sizes. These 20 tasks formed the testing data. The 20 objects in these testing tasks were different from the objects used in training. A total of five human subjects (four male and one female, aged between 20 and 30 years, and healthy without neurological disorders) were tested in this experiment. All these subjects were informed about the nature of the study and signed institutionally approved consent forms.

D. Analysis

First, we calculated angular velocities from the joint angle profiles collected in the experiment (see Fig. 2, for example). We truncated the entire profile to preserve only the relevant projectile movement—about 0.45 s or 39 samples under a sampling rate of 86 Hz.

Second, we constructed an angular velocity matrix X for each subject. As shown in Fig. 3, angular velocity profiles of the 15 joints corresponding to one object were cascaded, and each row of the angular velocity matrix represented one movement in time. The matrix had 40 rows and $39 \times 15 = 585$ columns

$$X = \begin{bmatrix} v_1^1(1) & \cdots & v_1^1(39) & \cdots & v_{15}^1(1) & \cdots & v_{15}^1(39) \\ \vdots & \vdots & \vdots & \vdots & \vdots & \vdots & \vdots \\ v_1^g(1) & \cdots & v_1^g(39) & \cdots & v_{15}^g(1) & \cdots & v_{15}^g(39) \\ \vdots & \vdots & \vdots & \vdots & \vdots & \vdots & \vdots \\ v_1^{40}(1) & \cdots & v_1^{40}(39) & \cdots & v_{15}^{40}(1) & \cdots & v_{15}^{40}(39) \end{bmatrix} \tag{5}$$

where $v_i^g(t)$ represents the angular velocity of joint i ($i = 1, \ldots, 15$) at time t ($t = 1, \ldots, 39$) in the gth grasping task ($g = 1, \ldots, 40$). Each row of the matrix X connects a start posture to an end posture. The velocity projectile describes the transformation from the start posture to the end posture. For a subject, as all movements started from the same hand posture, we can say that each row of the angular velocity matrix corresponds to one specific end posture. Note that in PCA and SVD, the data matrix is often arranged such that columns represent individual data samples, but in our case, it is the rows of matrix X that represent individual measurements—we have simply performed a transpose.

Third, we performed SVD on the angular velocity matrix X of each subject. We wrote X as follows:

$$X = U\Sigma Y \tag{6}$$

where U is a 40-by-40 matrix with orthonormal columns ($U'U$ equals an identity matrix), Y is a 40-by-585 matrix with orthonormal rows (YY' equals an identity matrix), and Σ is a 40-by-40 diagonal matrix denoted by $\mathrm{diag}\{\lambda_1, \lambda_2, \ldots, \lambda_{40}\}$ with

$\lambda_1 \geq \lambda_2 \geq \cdots \geq \lambda_{40} \geq 0$. For convenience of analysis in this paper, we used the aforementioned form of SVD (see [19, p. 44]), which is different from the standard form of SVD (where Y is square and Σ is of the same dimensions as X). We can approximate X by another matrix $\tilde{X}$ with reduced rank r by replacing Σ with $\mathrm{diag}\{\lambda_1, \ldots, \lambda_r, 0, \ldots, 0\}$. We can write the approximation matrix $\tilde{X}$ in a more compact form

$$\tilde{X} = U_r \,\mathrm{diag}\{\lambda_1, \ldots, \lambda_r\}\, Y_r \tag{7}$$

where U_r is a 40-by-r matrix containing the first r columns of U and Y_r is a r-by-585 matrix containing the first r rows of Y. Introducing a new symbol $W = U_r \,\mathrm{diag}\{\lambda_1, \ldots, \lambda_r\}$, we have

$$X \approx \tilde{X} = W Y_r. \tag{8}$$

Then, we call each row of Y_r as a PC and W as the weight matrix.

Fourth, we derived the kinematic synergies. We named the elements of Y_r in a way similar to (5)

$$Y_r \equiv \begin{bmatrix} y_1^1(1) & \cdots & y_1^1(39) & \cdots & y_{15}^1(1) & \cdots & y_{15}^1(39) \\ \vdots & \vdots & \vdots & \vdots & \vdots & \vdots & \vdots \\ y_1^r(1) & \cdots & y_1^r(39) & \cdots & y_{15}^r(1) & \cdots & y_{15}^r(39) \end{bmatrix} \tag{9}$$

and named the elements of W in the following way:

$$W = \begin{bmatrix} w_1^1 & \cdots & w_r^1 \\ \vdots & \ddots & \vdots \\ w_1^g & \cdots & w_r^g \\ \vdots & \ddots & \vdots \\ w_1^{40} & \cdots & w_r^{40} \end{bmatrix}. \tag{10}$$

According to (8), we can approximate each row of X by a linear combination of the r PCs. According to (8), (5), (9), and (10), we have

$$v_i^g(t) \approx \sum_{j=1}^{r} w_j^g y_i^j(t) \tag{11}$$

for $i = 1, \ldots, 15$, $g = 1, \ldots, 40$, and $t = 1, \ldots, 39$.

Since (11) has been written in the form of (4), we have found a solution to the synergy-extraction problem: The angular velocity profiles [obtained by rearranging all joints rowwise for the PCs—the reverse process of Fig. 3(a)]

$$\begin{bmatrix} y_1^j(1) & \cdots & y_1^j(39) \\ y_2^j(1) & \cdots & y_2^j(39) \\ \cdots & \cdots & \cdots \\ y_{15}^j(1) & \cdots & y_{15}^j(39) \end{bmatrix}, \qquad j = 1, \ldots, r$$

can be viewed as a set of candidates of the kinematic synergies. These kinematic synergies can serve as "building blocks" to reconstruct joint angular velocity profiles of hand movements [see (8) and (11)].

A comprehensive approach to decide r, the number of PCs or kinematic synergies, which are enough to reconstruct the testing postures, is presented in the next section. By linearly combining these synergies, 20 testing tasks were reconstructed. As we know the synergies and testing movement profiles, a least-squares method (pinv in MATLAB) was used to find the optimal linear combination of the kinematic synergies, which can reconstruct the testing movement profiles.

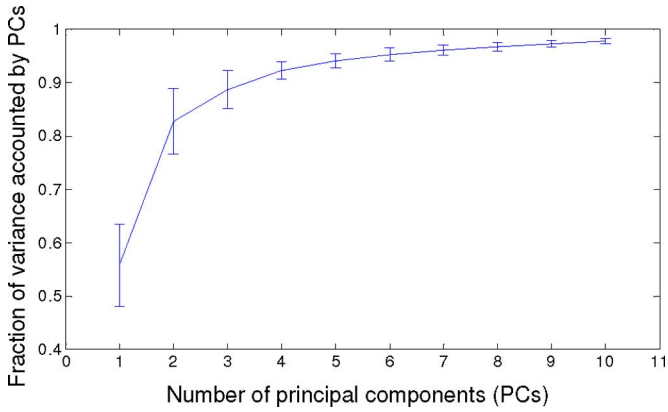

Fig. 4. Fraction of variance accounted by increasing number of PCs. Error bars indicate the standard deviation across subjects.

Fifth, we derived the temporal postural synergies from the kinematic synergies by integrating the angular velocity profiles of these kinematic synergies at the 15 joints from the initial posture.

III. Results

A typical task profile containing the velocity projectile is shown in Fig. 2. Note that the angular velocity profiles may have both positive and negative values corresponding to flexion and extension of a finger joint, respectively. It was observed that grasping tasks with different shaped objects often exhibited different patterns of joint coordination in the angular velocity profiles, while similar shaped objects of different sizes obtained similar patterns, but differed in amplitudes in the angular velocity profiles.

In the extraction of kinematic synergies or PCs using SVD, on average the first PC accounted for 56% of the total variance for all the five subjects. The first and second PCs together accounted for 82% of the total variance. In order to determine how many PCs would suffice to account for the variance of the entire training data, a PC-variation chart was plotted in Fig. 4. Error bars indicate standard deviation across the five subjects. Beyond six PCs, there was not much appreciable contribution of higher order PCs in the total variance. Note that this, by itself, might not be sufficient evidence to decide on the number of PCs or kinematic synergies. Another criterion used to determine the number of synergies is based on reconstruction errors (discussed later).

Angular velocity profiles of six kinematic synergies obtained for Subject 1 are depicted in Fig. 5. Across the rows are the 15 joints corresponding to the five fingers (three for each). These synergies show that peak velocities of the grasp occurred at the middle of the task. This reflects acceleration at the beginning of the task, which was generally open loop. It was followed by deceleration caused due error feedback from sensory and motor

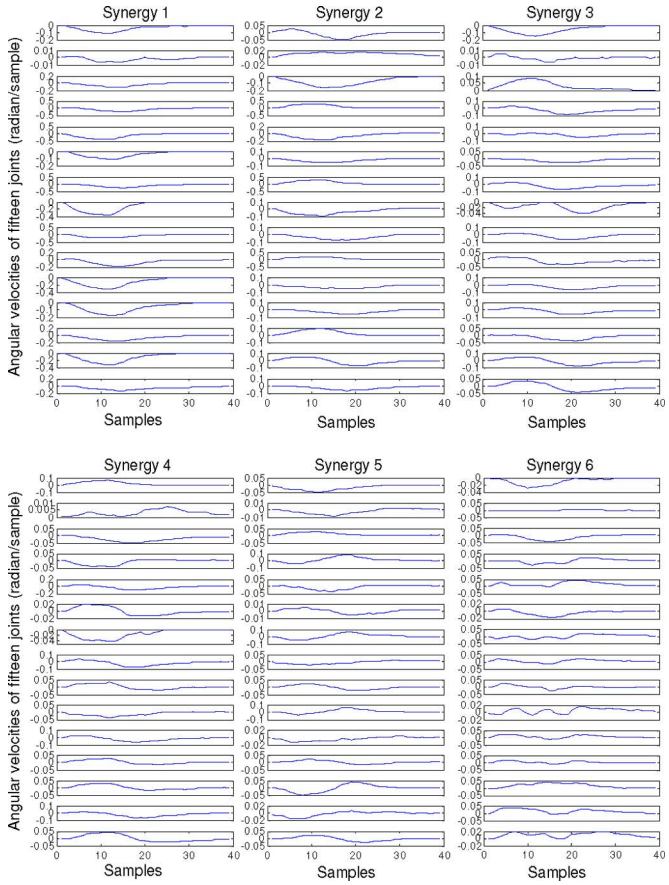

Fig. 5. Six kinematic synergies (39 samples at 86 Hz). Each synergy is about 0.45 s in duration.

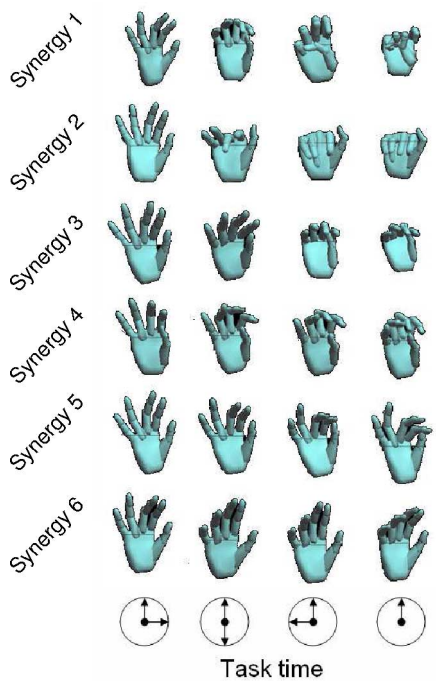

Fig. 6. Postural synergies of Subject 1. Each row corresponds to the temporal profile of one synergy. Each posture is a snapshot taken at discrete time steps (as indicated at the bottom of the figure) of the task. Synergies are arranged in the order of their significance with the first row (first synergy) being the most significant to the last row (last synergy) being the least significant. Note that end postures of the top two synergies are closed fists.

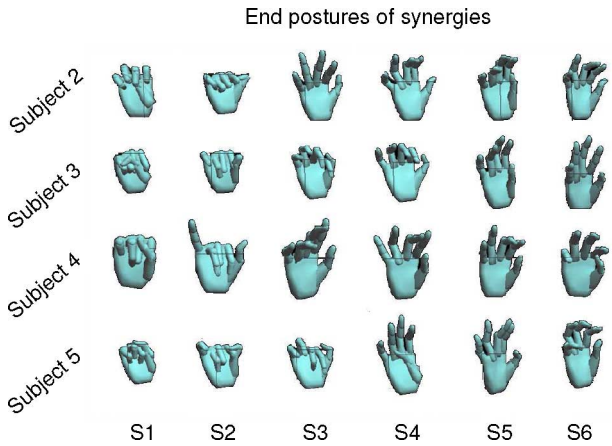

Fig. 7. Postural synergies of Subjects 2–5. Each row corresponds to the end postures of six different synergies (denoted S1, . . . , S6) for one subject in the decreasing order of their significance from left to right. End postures (rather than detailed temporal postures) for Subjects 2–5 are shown here.

systems while reaching the precise position of object, and finally closing of the grasp.

Given the initial posture, the temporal variation of postures along each kinematic synergy can be calculated via integration. A set of six such temporal postural synergies obtained from Subject 1 are depicted in Fig. 6. In the figure, four postures are snapshots at 25%, 50%, 75%, and 100% of the task times, respectively. End posture of each synergy indicates the contribution of synergy in a particular type of grasp. End postures of the six synergies for the remaining four subjects are shown in Fig. 7. As all the subjects performed tasks on the same training objects, there were similarities in synergies adapted, among the subjects. First two and last two synergies were very similar across all the subjects. The end postures of the third and fourth synergies were not the same for all the subjects although there were some similarities.

By linearly combining the synergies, for each subject 20 grasping tasks that comprise the testing data were reconstructed. One of the reconstructions is shown in Fig. 8. As clearly evident, the reconstruction was reasonably accurate using six synergies in the following task. The reconstruction errors in other cases can be seen in the reconstruction error plot illustrated in Fig. 9. The reconstruction errors were calculated for each subject and each task for various numbers of PCs by

$$\frac{\sum_{i=1}^{15}\sum_{t=1}^{39}\left[v_i^g(t)-\hat{v}_i^g(t)\right]^2}{\sum_{i=1}^{15}\sum_{t=1}^{39}v_i^g(t)^2}$$

where $\hat{v}_i^g(t)$ $(t=1,\ldots,39)$ is the angular velocity profile of task g and finger joint i $(i=1,\ldots,15)$ reconstructed using a given number of PCs. Note that the aforementioned reconstruction error is not a direct measure of the approximation error

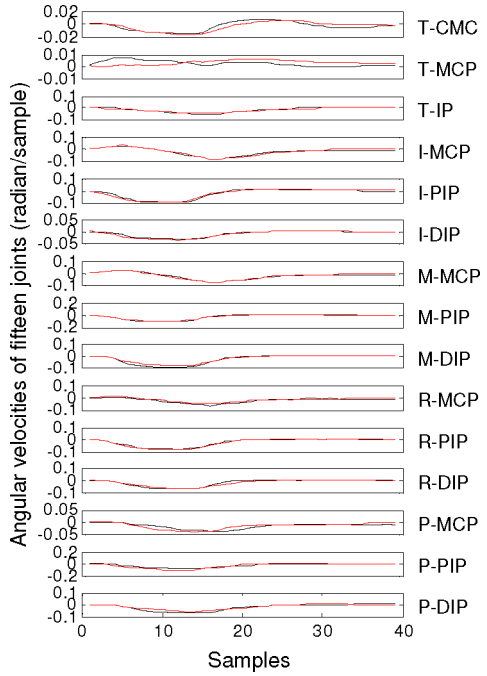

Fig. 8. Joint angular velocity profile of a grasping task (in black) is reconstructed (in red) by using six synergies for Subject 3.

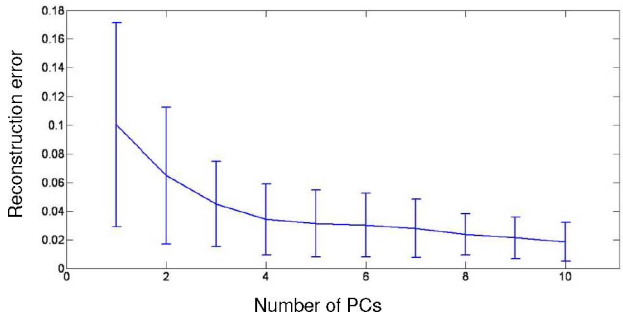

Fig. 9. Reconstruction error. The graph illustrates the gradual decrease in the reconstruction error while recruiting more synergies. Error bars indicate the standard deviation across subjects. This can also be used as a measure of calculating sufficient number of PCs.

(quadratic difference between the original and reconstructed angular velocity profiles), but expressed as a ratio between this approximation error and the size (also in quadratic sense) of the original angular velocity profiles. The error bars in Fig. 9 indicate standard deviation across subjects averaged across 20 testing tasks. The number of PCs versus reconstruction error plot also helps in determining the number of PCs. Although it is up to one's discretion about how many PCs can be considered to account for appreciable reconstruction, in our case six synergies were proved as sufficient for reconstruction of the testing tasks.

IV. Discussion

In this paper, kinematic synergies, and thereafter, temporal postural synergies were obtained based on a convolutive-mixture model for generation of hand movements. The model was reduced to a linear combination of synchronous synergies in rapid grasping tasks. The importance of these simple and higher level models lies in their instant applications in robotics, prosthetics, and rehabilitation. As these models are computationally inexpensive, they can be readily adapted for real-time applications in controlling prosthetic arms and hands with multiple DOF. Currently, such models are very much needed for rehabilitation and restoration of hand functions. For instance, single neuron recordings, made from monkey's motor cortex, have been used in decoding arm movement [20]. In such experiments, where only a few neurocommand signals and end kinematics are available, these high-level models will prove to be significantly helpful in predicting higher DOF with a few command signals.

The following anatomical insights were obtained from the temporal postural synergies. In Fig. 6, for the third, fourth, and fifth synergies in this subject, index finger acts as a master in leading the movement and rest of the fingers follow it as slaves. This concept has been observed previously and called enslaving [2]. Such biomechanical constraints can greatly reduce the complexity involved in controlling prosthetic hands. From the end postures in Figs. 6 and 7, it is clearly evident that no synergy is redundant and that they are all unique. The first synergy is a close fist. The second synergy can be used in tasks like holding a dice, the third synergy in holding small spheres, the fourth in holding cylindrical rods, the fifth in holding precision pinches, and the sixth in holding larger spheres/objects. In all of these synergies, as the size of the grasping object decreases, the flexion at metacarpal joints increases. In the first two synergies, the metacarpal flexion was dominant when compared to other synergies and gradually reduced for other synergies. Also, for major movements only MCP joints were involved. For precision movements after major movements, proximal and distal joints were recruited. This can be witnessed in the fifth synergy, suggesting hierarchical recruitment of joints. Similar findings will be reported in [17].

Temporal postural synergies play an important role in understanding the physiological aspects of the movement. Biologically inspired synergies have already taken an important place in prosthetics [21], [22]. In such technologically advancing scenarios, dominant static postures are by themselves not significant, unless they are supplied by the temporal information of how they can be achieved by collective coordination in different joints. In Fig. 6, the advantage of presenting the postural variation across time can be greatly appreciated. It is important to note here that intermediate postures may seem significant, but may not be physiologically meaningful. This implies that dominant static postures proposed earlier need not have physiological meaning. For example, in Fig. 6, intermediate posture at 50% time of the first synergy is almost similar to the end posture of the fourth synergy. Although the first synergy is aimed to grasp a tiny object, e.g., pearl, its intermediate posture looks very much like the fourth synergy that is targeted at grasping an object like cylindrical rod. Temporal postural synergies eliminate this ambiguity, as they supply the postural information across the time line of entire reach and grasp.

Not all people use the same set of strategies while grasping. Some studies considered common postural patterns across subjects, as synergies [8]. This leads us to a question, should all people use the same postural patterns and should these postural patterns be called synergies? Athletes, calligraphers, artists, and musicians have very sophisticated set of skills in hands, which can adapt to complex movements very easily, what to speak of day to day movements. Moreover, it was observed in [23] that fine finger movements improve over time and reflect the development of specialized neural connections in spinal cord. In such cases, synergies used by skilled professionals need not be the same as average class of people. The absence of common trends among different people does not mean the absence of synergies, but it means that people are adapting to a different set of synergies. Some synergies are innate, which might be common, but some are adaptive [24], as per the changes in environment.

The recruitment of these synergies implied that the synergy corresponding to full flexion had higher weight across all subjects. In all subjects, it was observed that on average the first synergy was also the synergy, which is mostly used in all the testing grasps. Note that the synergies were placed based on their contribution to the variance accounted in the testing data. The fact that the first synergy involved full flexion for all the subjects is in agreement with neurophysiology of movement. Next, in the order were the third, fourth, and fifth synergies, which were not the same for all subjects. Note that in the linear combinations of synergies to reconstruct testing grasps, negative coefficients were obtained for some synergies. What this means is by using the first synergy for full flexion and simultaneously, using the other synergies in opposite direction would inhibit the movement and enable the subject to achieve a range of various postures. This degree of inhibition can be controlled by the magnitude of the coefficients in the linear combination. This can be correlated to agonist and antagonist muscles acting simultaneously in opposite directions causing forward movement and at the same time deceleration by negative velocities to control the movement of hand in different tasks.

V. Conclusion

Kinematic synergies of the hand were extracted from a set of rapid grasping movements based on a simplified convolutive-mixture model for generation of hand movements. Carefully designed rapid grasping tasks enabled synchronous kinematic synergies to be obtained by SVD. The kinematic synergies were then translated into temporal postural synergies, which revealed interesting strategies of finger coordination. In this paper, we concentrated on determining the morphology of kinematic synergies in rapid hand movements, and in our future study, we will use the obtained synergies as templates to decompose the hand movements, so as to understand how the kinematic synergies are recruited in movement generation.

Acknowledgment

The authors would like to thank the reviewers and editors for their valuable suggestions and comments.

References

[1] N. Bernstein, *The Co-ordination and Regulation of Movements*. Oxford, U.K.: Pergamon, 1967.

[2] C. L. Mackenzie and T. Iberall, *The Grasping Hand (Advances in Psychology)*. Amsterdam, The Netherlands: North-Holland, 1994.

[3] M. Santello, M. Flanders, and J. F. Soechting, "Postural hand synergies for tool use," *J. Neurosci.*, vol. 18, no. 23, pp. 10 105–10 115, Dec. 1998.

[4] C. R. Mason, J. E. Gomez, and T. J. Ebner, "Hand synergies during reach-to-grasp," *J. Neurophysiol.*, vol. 86, no. 6, pp. 2896–2910, Dec. 2001.

[5] M. Santello, M. Flanders, and J. F. Soechting, "Patterns of hand motion during grasping and the influence of sensory guidance," *J. Neurosci.*, vol. 22, no. 4, pp. 1426–1435, Feb. 2002.

[6] T. E. Jerde, J. F. Soechting, and M. Flanders, "Biological constraints simplify the recognition of hand shapes," *IEEE Trans. Biomed. Eng.*, vol. 50, no. 2, pp. 265–269, Feb. 2003.

[7] E. Todorov and Z. Ghahramani, "Analysis of the synergies underlying complex hand manipulation," in *Proc. 26th Annu. Int. Conf. IEEE EMBS*, San Francisco, CA, Sep. 2004, pp. 4637–4640.

[8] P. H. Thakur, A. J. Bastian, and S. S. Hsiao, "Multidigit movement synergies of the human hand in an unconstrained haptic exploration task," *J. Neurosci.*, vol. 28, no. 6, pp. 1271–1281, Feb. 2008.

[9] I. V. Grinyagin, E. V. Biryukova, and M. A. Maier, "Kinematic and dynamic synergies of human precision-grip movements," *J. Neurophysiol.*, vol. 94, no. 4, pp. 2284–2294, Oct. 2005.

[10] R. Vinjamuri, Z.-H. Mao, R. Sclabassi, and M. Sun, "Time-varying synergies in velocity profiles of finger joints of the hand during reach and grasp," in *Proc. 29th Annu. Int. Conf. IEEE EMBS*, Lyon, France, Aug. 2007, pp. 4846–4849.

[11] A. d'Avella, A. Portone, L. Fernandez, and F. Lacquaniti, "Control of fast-reaching movements by muscle synergy combinations," *J. Neurosci.*, vol. 26, no. 30, pp. 7791–7810, Jul. 2006.

[12] M. L. Latash and J. G. Anson, "Synergies in health and disease: Relations to adaptive changes in motor coordination," *Phys. Therapy*, vol. 86, no. 8, pp. 1151–1160, Aug. 2006.

[13] E. Bizzi, "Motor primitives and rehabilitation," in *Proc. 6th Int. Workshop Virtual Rehabil.*, Venice, Italy, Sep. 2007, pp. 20–22.

[14] R. Vinjamuri, D. Crammond, D. Kondziolka, H.-N. Lee, and Z.-H. Mao, "Extraction of sources of tremor in hand movements of patients with movement disorders," *IEEE Trans. Inf. Technol. Biomed.*, vol. 13, no. 1, pp. 49–56, Jan. 2009.

[15] F. A. Mussa-Ivaldi, S. F. Giszter, and E. Bizzi, "Linear combination of primitives in vertebrate motor control," *Proc. Natl. Acad. Sci.*, vol. 91, no. 16, pp. 7534–7538, Aug. 1994.

[16] T. Flash and B. Hochner, "Motor primitives in vertebrates and invertebrates," *Curr. Opin. Neurobiol.*, vol. 15, no. 6, pp. 660–666, Dec. 2005.

[17] R. Vinjamuri, M. Sun, C.-C. Chang, H.-N. Lee, R. J. Sclabassi, and Z.-H. Mao, "Dimensionality reduction in control and coordination of the human hand," *IEEE Trans. Biomed. Eng.*, vol. 57, no. 2, pp. 284–295, Feb. 2010.

[18] Virtual Realities, Inc. Galveston, Texas, USA. (2009, Jul.). [Online]. Available: http://www.vrealities.com/cyber.html

[19] I. T. Jolliffe, *Principal Component Analysis,* 2nd ed. New York: Springer-Verlag, 2002.

[20] M. Velliste1, S. Perel, M. C. Spalding, A. S. Whitford, and A. B. Schwartz, "Cortical control of a prosthetic arm for self-feeding," *Nature*, vol. 453, no. 19, pp. 1098–1101, Jun. 2008.

[21] M. Popovic and D. Popovic, "Cloning biological synergies improves control of elbow neuroprostheses," *IEEE Eng. Med. Biol. Mag.*, vol. 20, no. 1, pp. 74–81, Jan./Feb. 2001.

[22] S. D. Iftime, L. L. Egsgaard, and M. B. Popovic, "Automatic determination of synergies by radial basis function artificial neural networks for the control of a neural prosthesis," *IEEE Trans. Neural Syst. Rehabil. Eng.*, vol. 13, no. 4, pp. 482–489, Dec. 2005.

[23] A. M. Wing, P. Haggard, and J. R. Flanagan, *Hand and Brain: The Neurophysiology and Psychology of Hand Movements*. San Diego, CA: Academic, 1996.

[24] M. B. Berkinblit, A. G. Feldman, and O. I. Fukson, "Adaptability of innate motor patterns and motor control mechanisms," *Behav. Brain Sci.*, vol. 9, no. 4, pp. 585–638, 1986.

Ramana Vinjamuri (S'02–M'08) received the B.S. degree in electrical and electronics engineering from Kakatiya University, Warangal, India, in 2002, the M.S. degree in electrical engineering (specialized in bioinstrumentation) from Villanova University, Villanova, PA, in 2004, and the Ph.D. degree in electrical engineering (specialized in dimensionality reduction techniques in hand movements, prosthesis, robotics, and virtual reality) from the University of Pittsburgh, Pittsburgh, PA, in 2008.

He is currently a Postdoctoral Fellow with the Department of Physical Medicine and Rehabilitation, University of Pittsburgh, where he is engaged in the field of neural prosthesis through brain–computer interface.

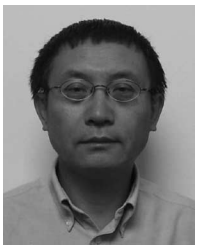

Mingui Sun (S'88–M'89–SM'05) received the B.S. degree from Shenyang Chemical Engineering Institute, Shenyang, China, in 1982, and the M.S. and Ph.D. degrees in electrical engineering from the University of Pittsburgh, Pittsburgh, PA, in 1986 and 1989, respectively.

Since 1991, he has been with the University of Pittsburgh, where he is currently a Professor of neurosurgery, electrical and computer engineering, and bioengineering. He is also the Director of Research with the Computational Diagnostics, Inc., Pittsburgh. His research interests include advanced biomedical electronic devices, biomedical signal and image processing, sensors and transducers, biomedical instruments, artificial neural networks, wavelet transforms, time–frequency analysis, and the inverse problem of neurophysiological signals. He has authored or coauthored more than 200 publications.

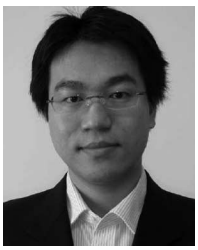

Cheng-Chun Chang (S'06–M'09) received the B.Sc. degree from National Tsing-Hua University, Hsinchu, Taiwan, China, in 2001, the M.Sc. degree from National Taiwan University, Taipei, Taiwan, China, in 2003, and the Ph.D. degree from the University of Pittsburgh, Pittsburgh, PA, in 2008, all in electrical engineering.

During 2005, he was a Postgraduate Student with Johns Hopkins University, Baltimore, MD. During 2009, he was a Principal Engineer with Nanolambda, where he was a Palso an In charge of algorithm development for applications of nanooptical-filter-array spectrum sensors. Since August 2009, he has been an Assistant Professor with the Department of Electrical Engineering, National Taipei University of Technology, Taipei. His current research interests include general area of digital signal processing, wireless communications, and the application of signal processing techniques to optical and biomedical applications.

Heung-No Lee (S'94–M'99) was born in Choong-Nam, Korea. He received the B.S., M.S., and Ph.D. degrees in electrical engineering from the University of California, Los Angeles, in 1993, 1994, and 1999, respectively.

From 1999 to 2001, he was with the Department of Network Analysis and Systems, Information Science Laboratory, Hughes Research Laboratories, Malibu, CA, where he was a Principal Investigator in a number of research projects. In 2002, he was as an Assistant Professor with the Department of Electrical Engineering, University of Pittsburgh, Pittsburgh, PA, where he started the Communications Research Laboratory in 2002 and was engaged in number of research projects as PI or co-PI supported by the National Science Foundation, Pittsburgh Digital Greenhouse (the Technology Collaborative), Adcus, and NanoLambda. Since 2009, he has been an Associate Professor with the Department of Information and Communications, Gwangju Institute of Science and Technology, Gwangju, Korea. His current research interests include information, channel coding, communications, and signal processing theories for wireless networking, and biomedical applications.

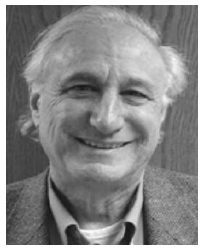

Robert J. Sclabassi (S'68–M'62–SM'93) received the B.S.E. degree in electrical engineering from Loyola University, Los Angeles, CA, the M.S.E.E. and Ph.D. degrees in electrical engineering from the University of Southern California, Los Angeles, and the M.D. degree in medicine from the University of Pittsburgh, Pittsburgh, PA.

He was with the Advanced Systems Laboratory, TRW, Los Angeles. He was a Postdoctoral Fellow with the Brain Research Institute, University of California, Los Angeles, where he was also a Faculty member with the Department of Neurology and Biomathematics. He is currently a Professor of neurological surgery, psychiatry, electrical engineering, mechanical engineering, and behavioral neuroscience with the University of Pittsburgh. He has authored or coauthored more than 400 papers, chapters, and conference proceedings.

Prof. Sclabassi is a Registered Professional Engineer.

Zhi-Hong Mao (S'96–M'05–SM'09) received the dual B.S. degrees in automatic control and applied mathematics and the M.Eng. degree in intelligent control and pattern recognition from Tsinghua University, Beijing, China, in 1995 and 1998, respectively, the S.M. degree in aeronautics and astronautics from Massachusetts Institute of Technology (MIT), Cambridge, in 2000, and the Ph.D. degree in electrical and medical engineering from the Harvard-MIT Division of Health Sciences and Technology, Cambridge, in 2005.

Since 2005, he has been an Assistant Professor with the Department of Electrical and Computer Engineering and the Department of Bioengineering, University of Pittsburgh, Pittsburgh, PA.